

Structural, Magnetic, and Electronic Properties of the Monometallofullerene Gd@C₈₂: Theory

Ali Sebetci* and Manuel Richter†

IFW Dresden, P.O. Box 270116, D-01171 Dresden, Germany

(Dated: November 23, 2018)

Abstract

The structural, electronic, and magnetic properties of Gd@C₈₂ endohedral metallofullerene have been studied by employing on-site correlation corrected, scalar-relativistic and full-relativistic density functional theory within the local density and generalized gradient approximations. The experimentally observed reduction of the magnetic moment of Gd@C₈₂ with respect to that of a free Gd⁺³ ion can be explained by a tiny hybridization between unoccupied Gd-4f states and carbon- π states, resulting in a generic antiferromagnetic coupling of the Gd-4f spin with the remaining unpaired spin in the hybridized molecular orbital.

PACS numbers: 71.20.Tx, 73.22.-f, 75.75.+a

Keywords: metallofullerene, magnetic properties, DFT

*Current affiliation: Department of Chemistry, University of California, Riverside, CA 92521 USA; Electronic address: sebetci@ucr.edu

†Electronic address: m.richter@ifw-dresden.de

I. INTRODUCTION

Rare-earth (RE) based metallofullerenes such as RE@C₆₀ [1], RE@C₈₂ [2], and RE₃N@C₈₀ [3] can be solvated in water and functionalized with poly- and multihydroxyl groups in order to be used as contrast enhancing agent for magnetic resonance imaging (MRI). Their advantage is not only that they are safer than the commercial MRI contrast agents such as Gd-DTPA since the toxic RE ions are totally encapsulated by the fullerenes and cannot escape from the cage under biological conditions but also that they can produce proton relaxivities nearly twenty times larger than those of the commercial agents [2, 4]. Proton relaxivity is the ability of magnetic compounds to increase the relaxation rates of the surrounding water proton spins.

Metallofullerenes are also promising in photoelectrochemical cell [5] and molecular memory [6, 7] applications as well as spintronics devices [8]. Therefore, endohedral monometallofullerenes of type RE@C₈₂, beside the others, have attracted a wide interest during the last decade [9, 10, 11, 12, 13, 14, 15, 16, 17]. Although there is a considerable number of investigations of these systems published, the structural and magnetic properties of monometallofullerenes and the details of the interaction between the metal atom and the carbon cage still need to be clarified.

The cage structures of Sc@C₈₂ [18] and La@C₈₂ [19] have been determined to have C_{2v} symmetry by a synchrotron radiation powder diffraction based structural analysis using the maximum entropy method (MEM). Inside the carbon cages, the RE atoms are located at an off-centre position adjacent to a carbon six-membered ring. This structure has been confirmed by ¹³C NMR spectroscopy [20]. The similarity in UV/vis/NIR spectra of 10 kinds of RE@C₈₂ (RE = La, Ce, Pr, Nd, Gd, Tb, Dy, Ho, Er, and Lu) [21] dissolved in toluene strongly suggests that Gd@C₈₂ possesses C_{2v} symmetry as Sc@C₈₂ and La@C₈₂. An extended X-ray absorption fine structure (EXAFS) study has proposed a position of the Gd ion in the C₈₂ cage above the carbon hexagon [22]. However, in a later experimental study, Nishibori *et al.* [23] have suggested, on the basis of synchrotron radiation powder structure MEM analysis, that the Gd atom would be located in the vicinity of the C-C double bond on the same C_2 molecular axis of the C₈₂ cage, but opposite to the six-membered ring where Sc and La atoms in Sc@C₈₂ and La@C₈₂ are known to be placed. On the theoretical side, it has been reported in an earlier density functional theory (DFT) calculation [11] that C₈₂-

C_{2v} cage symmetry is the most stable structure for La@C₈₂ metallofullerenes where La ions are strongly bonded to the hexagonal rings of the cages. In this study by Kobayashi and Nagase [11], structural relaxation of Gd@C₈₂ metallofullerene with different initial positions of the Gd atom in the cage was not considered. Later, Senapati *et al.* [24, 25, 26] have reported that their scalar relativistic DFT calculations with effective core potentials (ECP) did not agree with the MEM/Rietveld-based X-ray synchrotron powder diffraction structure of Nishibori *et al.* [23]. They have found the most stable position of the Gd atom adjacent to the C-C double bond but not on the C_2 molecular axis of the C₈₂ cage. Finally, the disagreement on the position of the Gd ion in the cage has been solved both theoretically and experimentally: Mizorogi and Nagase [27] performed DFT calculations and revealed that the so-called anomalous structures with Gd close to the double bond are unstable and do not correspond to energy minima, and Liu *et al.* [30] have shown by an X-ray absorption near-edge structure (XANES) study that the Gd ion lies above the hexagon on the C_2 axis, like La and Sc.

Effective magnetic moments μ_{eff} of RE@C₈₂ metallofullerenes have been measured by employing Superconducting Quantum Interference Device (SQUID) magnetometers for RE = La, Gd [9], RE = Gd, Tb, Dy, Ho, Er [12] and by soft X-ray magnetic circular dichroism (SXMCD) spectrometers for RE = Gd, Dy, Ho, Er [17]. It has been found that they are significantly smaller than those of the corresponding free RE³⁺ ions. The amount of the reduction in effective magnetic moment is different for each metallofullerene with a general trend that the higher the orbital momentum, the larger the magnitude of the reduction [12]. Particularly, the measured values of 6.90 μ_B [9], 6.91 μ_B [12], and 6.8±0.5 μ_B [17] for Gd@C₈₂, which were obtained by fitting the experimental data to the Curie-Weiss law, correspond to an approximately 13% reduction in the effective moment compared to the theoretical value of 7.94 μ_B of the free trivalent Gd ion. The case of Gd is simpler than that of other RE, since the Gd magnetic moment is almost completely spin-dominated. Thus, the effective moment can be related to the allowed spin multiplicities, $M = 2S+1$ which is even for Gd³⁺ and odd for Gd@C₈₂. Indeed, $\mu_{\text{eff}} = 7.94 \mu_B$ corresponds to $M = 8$ (Gd³⁺) while $\mu_{\text{eff}} = 6.93 \mu_B$ would correspond to $M = 7$ if a vanishing orbital contribution is presumed. Senapati *et al.* [24] have calculated the total energy difference between different spin multiplicities of Gd@C₈₂ resulting from ferromagnetic ($M = 9$) and antiferromagnetic ($M = 7$) arrangements of the Gd f-electrons and the remaining odd electron, and concluded

that $M = 7$ is the ground state. This agrees with the experimental result by Furukawa *et al.* [14] who estimated the energy difference between the two states to be 1.8 meV.

Later, however, using the GAUSSIAN 03 code and a hybrid exchange correlation functional (B3LYP), Mizorogi and Nagase [27] have found that the $M = 9$ state is 0.4 meV more stable than $M = 7$ state. This is in contradiction with experiment.

The latter authors argued that Senapati *et al.* [24] obtained their conclusion only for one of the anomalous positions [25, 26]. In addition, we note that in all previous calculations on Gd@C₈₂ the Gd-4f-electrons were treated without any on-site correlation correction. Such corrections are obligatory for a decent description of 4f states in most rare-earth elements [28] and have been applied, e.g., to the 4f states of Gd@C₆₀ [29] recently.

In this work, our aim is to investigate the origin of the $M = 7$ ground state of Gd@C₈₂ theoretically. Starting from local spin density (LSDA) and generalized gradient approximations (GGA), we include on-site correlation correction, spin-orbit coupling, and non-collinearity effects in the DFT calculations which were not considered in any of the above mentioned previous theoretical approaches.

II. COMPUTATIONAL DETAILS

Three DFT codes have been used in our investigation: NWChem [31], FPLO-7.28 [32], and OpenMX [33]. This has become necessary as none of the codes includes all technical prerequisites to solve the problem.

Scalar-relativistic geometry optimizations without any on-site correlation correction have been performed with the program package NWChem to compare with results given in the literature. Then, the effect of on-site correlation corrections on the geometry has been studied by OpenMX. It turns out, that both methods give similar results but the OpenMX geometry data slightly deviate from the experimentally observed C_{2v} symmetry. Thus, we used the NWChem geometry data in the further calculations despite the fact that they were obtained by calculations without on-site correlation corrections.

The magnetic ground state has been investigated using on-site correlation corrected calculations with the FPLO code in scalar-relativistic mode. We also carried out the final analysis of the electronic structure with this code in order to clarify the origin of the observed antiferromagnetic coupling. In addition, the effect of spin-orbit coupling and non-collinear

magnetic moments has been checked with the OpenMX code.

In the calculations with NWChem, the hybrid functional B3LYP [34] has been chosen as the exchange-correlation functional, since this functional is known to provide geometries close to experiment in carbon systems. The scalar-relativistic effective core potential (ECP) and basis set developed by Cundari and Stevens [35] were used for Gd where the 46 inner electrons are replaced by the ECP and the outer $4f^7 5s^2 5p^6 5d^1 6s^2$ electrons are treated in the valence region. The split-valence d-polarized 3-21G* basis set was used for C.

The program package OpenMX [33] is based on norm-conserving pseudopotentials [36] and pseudo-atomic localized basis functions. In the calculations with OpenMX, the same outer electrons of the Gd atom (as in the NWChem calculations) were treated as valence electrons in the self consistent field iterations. The pseudo-atomic orbitals have been constructed by minimal basis sets (two-s, one-p, one-d, and one-f for Gd, and one-s, and one-p for C) within 8.0 Bohr radii cutoff radius of the confinement potential for Gd and 5.0 Bohr radii for C. The GGA+U approach [37] was applied in the atomic limit version in order to describe the correlated behavior of the Gd-4f shell. A value of $U-J = 7.2$ eV was used and the GGA functional was parameterized according to PBE [38]. A similar value, $U = 7.6$ eV, was recently used in a similar calculation for Gd@C₆₀ [29]. The cutoff energy for the real-space grid integration in the construction of the density matrix elements [39] has been chosen as 500 Ryd. The convergence criteria chosen were 0.1 μ Ha for the total energy and 0.1 mHa/Bohr for the geometry optimization.

The program FPLO is a full-potential all-electron local orbital code. It employs a fixed orbital basis with 4f, 5s5p5d5f, 6s6p6d, 7s valence orbitals for Gd and 1s, 2s2p, 3s3p3d valence orbitals for C. The LDA+U approach in the atomic limit version was applied with different values of U and $J = 0.8$ eV. The LDA functional was parameterized according to Perdew and Zunger [40].

III. RESULTS AND DISCUSSION

A. Geometric Structure

Let us recall: It is reported in a powder diffraction based structural analysis [23] that the endohedral structure of Gd@C₈₂ is anomalous, namely it is not the same as previously de-

terminated structures of La@C₈₂ and Sc@C₈₂. In addition, not the same anomalous structure suggested by the experiment but yet another anomalous structure has been predicted by DFT calculations [24, 25, 26]. However, most recently Liu *et al.* [30] have shown by XANES that Gd@C₈₂ has a normal endohedral structure. Furthermore, Mizorogi and Nagase [27] revealed by DFT calculations that the anomalous structures are unstable.

Our calculations support the findings of the most recent theoretical and experimental investigations. We have optimized the geometry of Gd@C₈₂ by NWChem and obtained a structure with C_{2v} symmetry (see Fig. 1) where the Gd atom sits at the centre of one of the hexagonal carbon rings. The optimized coordinates of the inequivalent atoms can be found in Table I. The calculated Gd-C bond length is 2.49 Å, while C-C bond lengths amount to 1.46 and 1.49 Å. In Ref. [27], using the same exchange-correlation functional, the Gd-C bond length was calculated as 2.47 Å. OpenMX optimization by GGA+U yields a very similar structure where the Gd atom locates at a position slightly off the centre of the ring. OpenMX calculations also reveal that the previously suggested two anomalous geometries have nearly 1.74 eV higher energies than the ground state structure.

B. Magnetic Properties

The magnetic moment of the unpaired electron in the hybrid orbital can couple with that of the seven Gd-4f electrons either ferromagnetically or antiferromagnetically. While the parallel arrangement corresponds to $M = 9$ for the metallofullerene, the antiparallel arrangement results in $M = 7$. The measured values of the effective magnetic moment of Gd@C₈₂ correspond to the $M = 7$ state. Furukawa *et al.* [14] have determined experimentally that the antiferromagnetic arrangement has 1.8 meV lower energy than the ferromagnetic one. On the other hand, Curie-Weiss law fitted experimental data by Funasaka *et al.* [9] and by Huang *et al.* [12] suggest that the antiferromagnetic arrangement is stable up to room temperature.

The inclusion of on-site correlation effects is mandatory for a correct description of the Gd-4f states and their influence on magnetic properties [28]. We have calculated the energy differences between the two magnetic states in LSDA+U approximation, using the FPLO code. Reasonable values of U for 4f states of neutral rare-earth atoms range between 6 eV and 7 eV [41]. These values are expected to be somewhat enhanced in a cationic situation

due to related orbital contraction. Therefore, we considered the range $U = 8, 10, \text{ and } 12$ eV. All considered values yield an $M = 7$ ground state, in accordance with the experiment. The $M = 9$ state lies 9 (3, 0.3) meV higher in energy for $U = 8$ (10, 12) eV. The related spin moments for all inequivalent atoms are given in Table I.

The influence of spin-orbit coupling and non-collinear spin arrangement on the relative positions of $M = 7$ and $M = 9$ states has been checked with the OpenMX code. Both effects produce only marginal changes and can be neglected.

C. Electronic Structure

The electron energy levels of the $\text{Gd}@C_{82}$ metallofullerene close to the chemical potential, obtained by the FPLO code in scalar-relativistic mode and using LSDA+U, $U = 8$ eV, are shown in Fig. 2 for $M = 7$ and $M = 9$. There is one almost spin-degenerate level at the chemical potential, well separated from the next lower occupied and next higher unoccupied levels by about 0.6-0.7 eV. In the antiferromagnetic $M = 7$ ground state, the HOMO is in the spin-down channel and the LUMO in the spin-up channel. The opposite situation is found in the ferromagnetic $M = 9$ state.

The occupied 4f levels (spin-up by definition) are situated at ~ -16 eV, about 11 eV below the chemical potential and outside the displayed energy range in Fig. 2. Thus, they are chemically inert and only contribute a spin magnetic moment. The calculated position of the occupied 4f levels agrees with the recent photoemission data of $\text{Gd}@C_{60}$ locating the 4f emission at a -10 to -11 eV binding energy [29]. The unoccupied 4f-spin-down levels are separated from the 4f-spin-up levels by the sum of exchange splitting (about 5 eV in the Gd-4f shell) and the term $U-J$. Thus, they are situated at ~ -4 eV, about 1 eV above the chemical potential.

The 6s and 5d electrons of the Gd atom essentially occupy empty states of the carbon cage, since the chemical potential of the empty cage lies below the Gd chemical potential. However, Mulliken population analysis shows a Gd occupation of $4f^{7.02}5d^{1.16}6s^{0.07}$ in the metallofullerene. The 5d occupation indicates a non-negligible degree of covalency. Indeed, population analysis of the individual π -like molecular orbitals reveals a 5d contribution in the percent range.

What might be more interesting is a 4f contribution of about 1 percent to the (spin-down)

HOMO of the $M = 7$ ground state and to the (spin-down) LUMO of the $M = 9$ state. Such a contribution is not present in the spin-up channel (LUMO of the $M = 7$ ground state and HOMO of the $M = 9$ state), since the 4f-spin-up states are inert. This difference provides an explanation for the observed and also calculated lower energy of the $M = 7$ state: Due to the position of the unoccupied 4f-spin-down states close to the chemical potential, more variational freedom is available for the spin-down molecular orbitals and their energy is reduced with respect to the spin-up levels, thus favoring a spin-down HOMO and a related antiferromagnetic coupling between the Gd-4f shell and the unpaired electron at the cage. Using a simplifying two-level model, one can roughly estimate the lowering of the spin-down level closest to the chemical potential by interaction with the 4f states:

$$\varepsilon_{\text{hyb}}^{\downarrow} - \varepsilon_{\pi} \approx -\frac{(\varepsilon_{4f}^{\downarrow} - \varepsilon_{\pi})^2 |C_{4f}^{\downarrow}|^2}{\varepsilon_{4f}^{\downarrow} - \varepsilon_{\pi}}$$

Here, $\varepsilon_{\text{hyb}}^{\downarrow}$ and ε_{π} denote the level of the 4f- π hybrid and the pure π state, respectively, $\varepsilon_{4f}^{\downarrow}$ denotes the position of the empty 4f state, and $|C_{4f}^{\downarrow}|^2$ denotes the squared 4f contribution to the eigenvector of the hybrid state. The latter amounts to about 1% for $U = 8$ eV. Using $\varepsilon_{4f}^{\downarrow} - \varepsilon_{\pi} \approx 1$ eV, we arrive at a level lowering in the order of 10 meV, accounting for the calculated energy difference between $M = 7$ and $M = 9$ states, 9 meV. This energy difference is reduced, if U is enhanced but stays positive up to the (unreasonably high) value of $U = 12$ eV.

A final remark is in place to explain the relative position of HOMO and LUMO in the ferromagnetic state. If $M = 9$ is forced in the calculation, the spin-up molecular orbital at the chemical potential is occupied. The related spin density (mainly situated on the carbon cage, see inset of Fig. 2) creates an exchange field that lowers the position of the spin-up level. The same happens in the $M = 7$ case for the spin-down level. Both shifts are due to (unphysical) self-exchange of the unpaired electron on the cage. In the latter case, the spin-down level was anyway lower in energy than the spin-up level due to 4f- π hybridisation, and self-exchange enhances the splitting between the two levels. In the $M = 9$ case, self-exchange and hybridisation effects compete and the level splitting is lower than in the $M = 7$ case. Though the total energy is slightly shifted by the described effect in an unphysical manner, this shift is virtually equal in the $M = 7$ and the $M = 9$ state and hence does not influence the energy difference between these states.

IV. CONCLUSIONS

In the present study, the structural, magnetic, and electronic properties of Gd@C₈₂ endohedral metallofullerene have been investigated by different approximations within density functional theory. It is confirmed that the lowest energy structure of Gd@C₈₂ has C_{2v} symmetry where the Gd atom is located at a position on the symmetry axis, adjacent to a carbon six-membered ring. The highest molecular orbitals of Gd@C₈₂ are not pure π states but (4f)-d- π hybridized molecular orbitals. The experimentally observed reduction of the Gd@C₈₂ magnetic moment with respect to that of a free Gd⁺³ ion is due to antiferromagnetic coupling between the 4f electrons of the Gd atom and the remaining unpaired electron on the hybridized molecular orbital. The reason for this antiferromagnetic coupling is a small hybridization of the unoccupied 4f-spin-down states with the carbon π -states. It yields an $M = 7$ ground state that should be generic for all Gd-carbon systems with unpaired electrons. For example, an $M = 7$ ground state has also been found for Gd@C₆₀ in a recent calculation [29].

Acknowledgments

We like to thank Alexey Popov, Klaus Koepernik, Helmut Eschrig, Gotthard Seifert, and Lothar Dunsch for discussions. Financial support has been provided by the German Science Foundation via SPP 1145.

-
- [1] Bolskar, R.D.; Benedetto, A.F.; Husebo, L.O.; Price, R.E.; Jackson, E.F.; Wallace, S.; Wilson, L.J.; Alford, J.M. *J. Am. Chem. Soc.* **2003**, *125*, 5471.
 - [2] Kato, H.; Kanazawa, Y.; Okumura, M.; Taninaka, A.; Yokawa, T. Shinohara, H. *J. Am. Chem. Soc.* **2003**, *125*, 4391.
 - [3] Fatouros, P.P.; Corwin, F.D.; Chen, Z.J.; Broaddus, W.C.; Tatum, J.L.; Kettenmann, B.; Ge, Z.; Gibson, H.W.; Russ, J.L.; Leonard, A.P.; Duchamp, J.C.; Dorn, H.C. *Radiology* **2006**, *240*, 756.
 - [4] Zhang, E.Y.; Shu, C.Y.; Feng, L.; Wang, C.R. *J. Phys. Chem. B* **2007**, *111*, 14223.
 - [5] Yang, S.; Fan, L.; Yang, S. *J. Phys. Chem. B* **2004**, *108*, 4394.

- [6] Slanina, Z.; Kobayashi, K.; Nagase, S. *Nanotech 2004, Technical Proceedings of the 2004 NSTI Nanotechnology Conference and Trade Show; Laudon, M. Romanowicz, B., Eds.; Computational Publications: Cambridge, MA 2004, Vol. 3.*
- [7] Jones, A.A.G.; Morton, J.J.L.; Taylor, R.A.; Ardavan, A.; Briggs, G.A.D. *Phys. Stat. Sol.* **2006**, *243*, 3037.
- [8] Shimada, T.; Okazaki, T.; Taniguchi, R.; Sugai, T.; Shinohara, H.; Suenaga, K.; Ohno, Y.; Mizuno, S.; Kishimoto, S.; Mizutani, T. *Appl. Phys. Lett.* **2002**, *81*, 4067.
- [9] Funasaka, H.; Sugiyama, K.; Yamamoto, K.; Takahashi, T. *J. Phys. Chem.* **1995**, *99*, 1826.
- [10] Kessler, B.; Bringer, A.; Cramm, S.; Schlebusch, C.; Eberhardt, W.; Suzuki, S.; Achiba, Y.; Esch, F.; Barnaba, M.; Cocco, D. *Phys. Rev. Lett.* **1997**, *79*, 2289.
- [11] Kobayashi, K.; Nagase, S. *Chem. Phys. Lett.* **1998**, *282*, 325.
- [12] Huang, H.; Yang, S.; Zhang, X. *J. Phys. Chem. B* **2000**, *104*, 1473.
- [13] Suenaga, K.; Iijima, S.; Kato, H.; Shinohara, H. *Phys. Rev. B* **2000**, *62*, 1627.
- [14] Furukawa, K.; Okubo, S.; Kato, H.; Shinohara, H.; Kato, T. *J. Phys. Chem. A* **2003**, *107*, 10933.
- [15] De Nadai, C.; Mirone, A.; Dhesi, S.S.; Bencok, P.; Brookes, N.B.; Marenne, I.; Rudolf, P.; Tagmatarchis, N.; Shinohara, H.; Dennis, T.J.S. *Phys. Rev. B* **2004**, *69*, 184421.
- [16] Bondino, F.; Cepek, C.; Tagmatarchis, N.; Prato, M.; Shinohara, H.; Goldoni, A. *J. Phys. Chem. B* **2006**, *110*, 7289.
- [17] Kitaura, R.; Okimoto, H.; Shinohara, H.; Nakamura, T.; Osawa, H. *Phys. Rev. B* **2007**, *76*, 172409.
- [18] Nishibori, E.; Takata, M.; Sakata, M.; Inakuma, M.; Shinohara, H. *Chem. Phys. Lett.* **1998**, *79*, 298.
- [19] Nishibori, E.; Takata, M.; Sakata, M.; Tanaka, H.; Hasegawa, M.; Shinohara, H. *Chem. Phys. Lett.* **2000**, *330*, 497.
- [20] Akasaka, T.; Wakahara, T.; Nagase, S.; Kobayashi, K.; Waelchli, M.; Yamamoto, K.; Kondo, M.; Shirakura, S.; Okubo, S.; et al. *J. Am. Chem. Soc.* **2000**, *122*, 9316.
- [21] Akiyama, K.; Sueki, K.; Kodama, T.; Kikuchi, K.; Ikemoto, I.; Katada, M.; Nakahara, H. *J. Phys. Chem. A* **2000**, *104*, 7224.
- [22] Giefers, H.; Nessel, F.; Györy, S.I.; Strecker, M.; Wortmann, G.; Grushko, Y.S.; Alekseev, E.G.; Kozlov, V.S. *Carbon* **1999**, *37*, 721.

- [23] Nishibori, E.; Iwata, K.; Sakata, M.; Takata, M.; Tanaka, H.; Kato, H.; Shinohara, H. *Phys. Rev. B* **2004**, *69*, 113412.
- [24] Senapati, L.; Schrier, J.; Whaley, K.B. *Nano Lett.* **2004**, *4*, 2073.
- [25] Wang, L.; Yang, D. *Nano Lett.* **2005**, *5*, 2340.
- [26] Senapati, L.; Schrier, J.; Whaley, K.B. *Nano Lett.* **2005**, *5*, 2341.
- [27] Mizorogi, N.; Nagase, S. *Chem. Phys. Lett.* **2006**, *431*, 110.
- [28] Richter, M. *J. Phys. D: Applied Physics* **1998**, *31*, 1017.
- [29] Sabirianov, R.F.; Mei, W.N.; Lu, J.; Gao, Y.; Zeng, X.C.; Bolskar, R.D.; Jeppson, P.; Wu, N.; Caruso, A.N.; Dowben, P.A. *J. Phys.: Condens. Matter* **2007**, *19*, 082201.
- [30] Liu, L.; Gao, B.; Chu, W.; Chen, D.; Hu, T.; Wang, C.; Dunsch, L.; Marcelli, A.; Luo, Y.; Wu, Z. *Chem. Commun.* **2008**, 474.
- [31] Bylaska, E.J.; de Jong, W.A.; Kowalski, K.; Straatsma, T.P.; Valiev, M.; Wang, D.; Apra, E.; Windus, T.L.; Hirata, S.; et al. "NWChem, A Computational Chemistry Package for Parallel Computers, Version 5.0" **2006**, Pacific Northwest National Laboratory, Richland, Washington 99352-0999, USA.
- [32] Koepernik, K.; Eschrig, H.; *Phys. Rev. B* **1999** *59*, 1743; <http://www.fplo.de>
- [33] Ozaki, T. *Phys. Rev. B* **2003**, *67*, 155108; Ozaki, T.; Kino, H. *Phys. Rev. B* **2004**, *69*, 195113; *Phys. Rev. B* **2005**, *72*, 045121.
- [34] Becke, A.D.; *J. Chem. Phys.* **1993** *98*, 5648.
- [35] Cundari, T.R.; Stevens, W.J. *J. Chem. Phys.* *98*, 1993 5555.
- [36] Troullier, N.; Martins, J.L. *Phys. Rev. B* **1991**, *43*, 1993.
- [37] Han, M.J.; Ozaki, T.; Yu, J. *Phys. Rev. B* **2006**, *73*, 045110.
- [38] Perdew, J.P.; Burke, K.; Ernzerhof, M. *Phys. Rev. Lett.* **1996**, *77*, 3865.
- [39] Ozaki, T.; Kino, H. *Phys. Rev. B* **2005**, *72*, 045121.
- [40] Perdew, J.P.; Zunger, A. *Phys. Rev. B* **1981**, *23*, 5048.
- [41] Richter, M. *Density Functional Theory applied to 4f and 5f Elements and Metallic Compounds, in: Handbook of Magnetic Materials (Ed. K.H.J. Buschow), Vol. 13, Elsevier, Amsterdam 2001* pp. 87–228.

TABLE I: Coordinates and spin moments for all inequivalent atoms of Gd@C₈₂. The coordinates originate from geometry optimization using NWChem with the B3LYP functional. The moments were obtained at the given coordinates by FPLO with LSDA+U using the PZ-81 functional and $U = 8$ eV, $J = 0.8$ eV.

Number	Atom	Coordinates (\AA)			Spin Moments (μ_B)	
		X	Y	Z	M = 9	M = 7
1	Gd	0.000	0.000	1.822	7.143	7.119
2	C	-1.215	3.943	0.643	0.002	-0.004
3	C	0.000	3.853	1.368	0.000	0.002
4	C	0.000	3.068	2.573	-0.010	-0.003
5	C	1.213	4.018	-0.789	0.025	-0.028
6	C	0.000	3.960	-1.534	-0.005	0.005
7	C	2.387	3.182	1.064	0.032	-0.037
8	C	2.354	2.368	2.217	-0.003	0.006
9	C	1.160	2.363	3.026	0.012	-0.022
10	C	3.108	1.166	2.198	0.000	0.002
11	C	2.408	2.669	-2.458	0.025	-0.028
12	C	2.400	3.325	-1.252	0.007	-0.008
13	C	3.091	2.754	-0.121	-0.001	0.001
14	C	3.687	1.465	-0.207	0.003	-0.003
15	C	3.764	0.720	1.004	0.025	-0.028
16	C	-1.205	2.652	-3.285	-0.005	0.006
17	C	0.000	3.256	-2.829	-0.000	-0.000
18	C	2.661	0.000	2.943	0.016	-0.029
19	C	1.512	0.000	3.803	-0.000	-0.029
20	C	0.743	1.238	3.847	-0.021	-0.017
21	C	3.097	1.406	-2.599	0.034	-0.037
22	C	3.660	0.735	-1.481	0.014	-0.015
23	C	-1.203	-1.426	-4.021	0.035	-0.039
24	C	-2.403	-0.683	-3.638	-0.003	0.004
25	C	0.000	-0.739	-4.330	-0.005	0.006

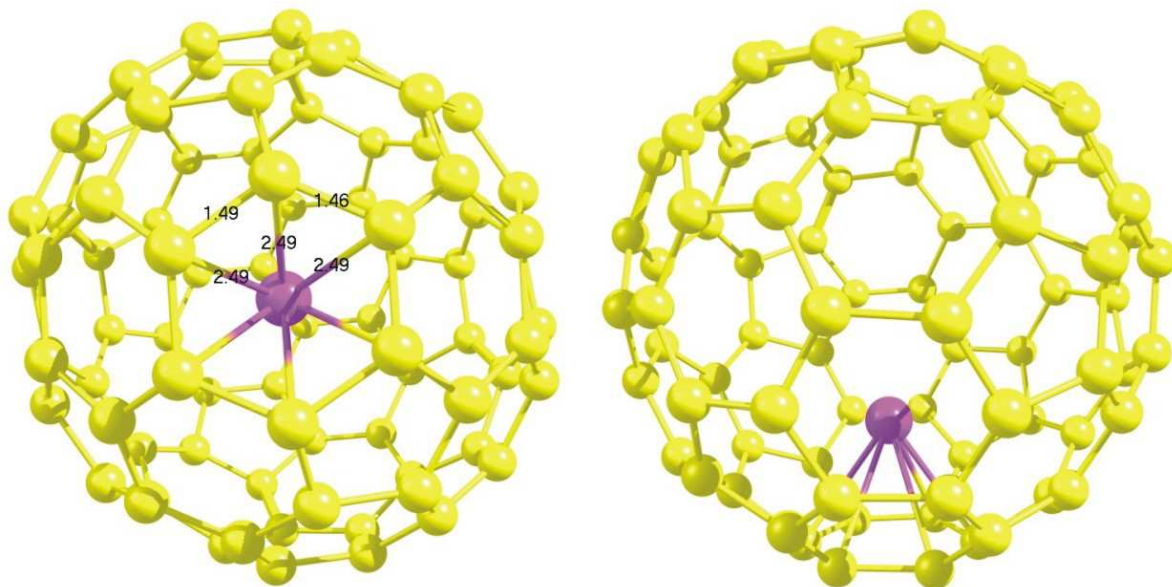


FIG. 1: (Color online) Top and side views of Gd@C₈₂ (relaxed structure). Distances are given in Å.

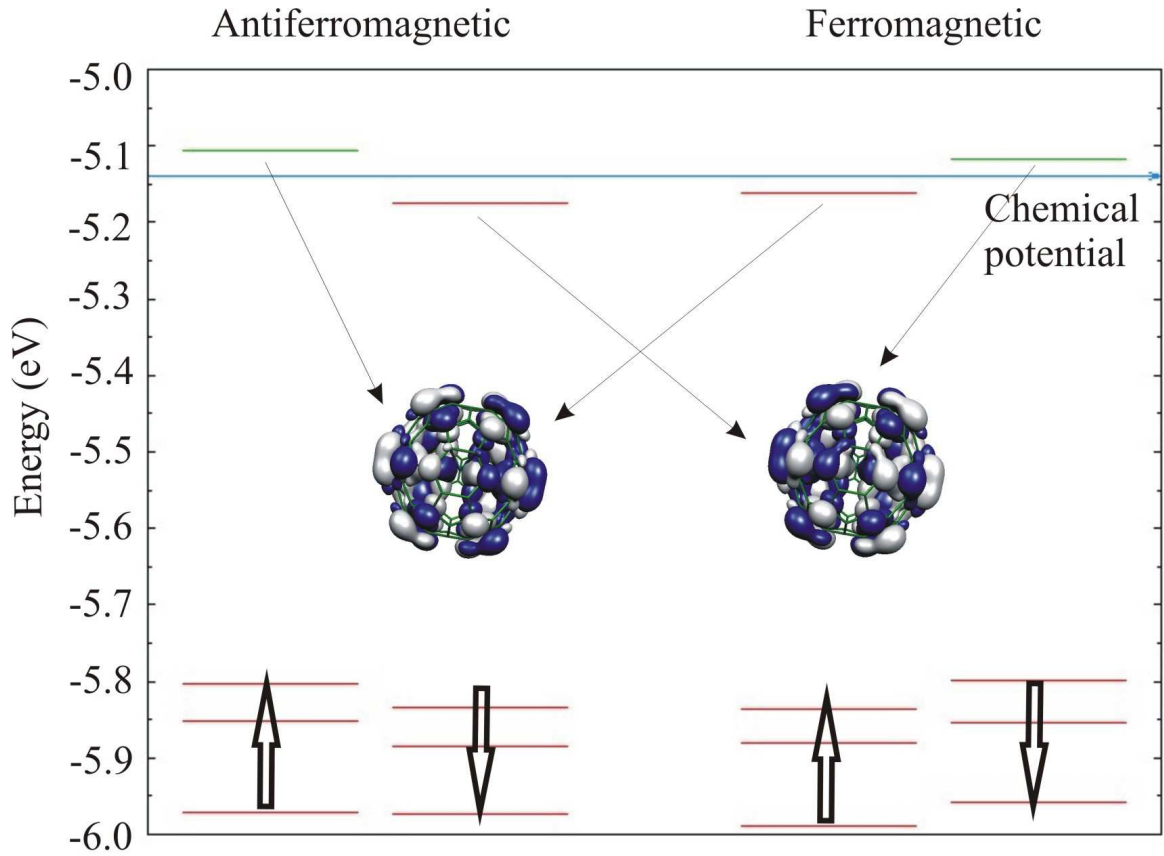


FIG. 2: Single electron energy levels of Gd@C₈₂ for the antiferromagnetic ($M = 7$) and ferromagnetic ($M = 9$) arrangements, obtained by scalar-relativistic LSDA+U calculations using the FPLO code, $U = 8$ eV. Dark (red online) and light lines (green online) represent occupied and unoccupied electron energy levels, respectively. The dark (blue online) and the light (gray online) areas in the density pictures represent positive and negative values of the related HOMO and LUMO wave function. It is hard to see the Gd contribution on these pictures since it amounts to about 1.5% only.